ADP-03-145/T584

DESY-03-207

Hybrid Meson Spectrum from the FLIC action

J.N. Hedditch[a], D. B. Leinweber[a], A. G. Williams[a] and J. M. Zanotti[ab]

[a]Special Research Center for the Subatomic Structure of Matter, and
Department of Physics, University of Adelaide Adelaide SA 5005 Australia

[b]John von Neumann-Institut für Computing NIC,
Deutsches Elektronen-Synchrotron DESY, D-15738 Zeuthen, Germany

The spectral properties of hybrid meson interpolating fields are investigated. The quantum numbers of the meson are carried by smeared-source fermion operators and highly-improved chromo-electric and -magnetic field operators composed with APE-smeared links. The effective masses of standard and hybrid operators indicate that the ground state meson is effectively isolated using both standard and hybrid interpolating fields. Focus is placed on interpolating fields in which the large spinor components of the quark and antiquark fields are merged. In particular, the effective mass of the exotic 1^{-+} meson is reported. Further, we report some values for excited mesonic states using a variational process.

1. INTRODUCTION

Major experimental efforts are currently aimed at determining the possible existence of exotic mesons; mesons having quantum numbers that cannot be carried by the minimal Fock space component of a quark-antiquark pair. Of particular mention is the proposed program of the GlueX collaboration associated with the forthcoming upgrade of the Jefferson Laboratory facility. The observation of exotic states and the determination of their properties would elucidate aspects of QCD which are relatively unexplored.

The quantum numbers $J^{PC} = 0^{+-}$, 0^{--}, 1^{-+}, etc. cannot be carried by a quark-antiquark pair in a ground-state S-wave. Lattice QCD calculations exploring the non-trivial role of explicit gluon degrees of freedom in carrying the quantum numbers of the meson suggest that exotic meson states do indeed exist and have a mass the order of 2 GeV [1]. These findings are further supported here.

2. SIMULATION METHODOLOGY

Operators carrying exotic quantum numbers can be constructed by merging standard local interpolating fields $\overline{q}^a(x)\Gamma q^a(x)$ with chromo-electric, $E_i^{ab}(x)$, or chromo-magnetic fields, $B_i^{ab}(x)$. The J^{PC} quantum numbers of the interpolator are derived from the direct product of those associated with the quark bilinear and E_i^{ab} (1^{--}) or B_i^{ab} (1^{+-}). For example, combining the vector current of the ρ meson with a chromo-magnetic field, $1^{--} \otimes 1^{+-}$ provides $0^{-+} \oplus 1^{-+} \oplus 2^{-+}$ with the 0^{-+}: $\bar{q}^a\gamma_i q^b B_i^{ab}$ (π meson) and the 1^{-+}: $\epsilon_{ijk}\bar{q}^a\gamma_i q^b B_j^{ab}$ (**exotic**). We restrict ourselves to the lowest energy-dimension operators, as these provide better signal with smaller statistical errors. Table 1 summarizes the standard and hybrid interpolating fields explored herein.

The formulation of effective interpolating fields for the creation and annihilation of exotic meson states continues to be an active area of research.

For example, one can generalize the structure of the interpolating fields further to include nonlocal components where link paths are incorporated to maintain gauge invariance and carry the nontrivial quantum numbers of the gluon fields. In this case, numerous quark propagators are required for each gauge field configuration rendering the approach computationally expensive.

Here we consider local interpolating fields. Gauge-invariant Gaussian smearing [2,3] is applied at the fermion source ($t = 3$), and local sinks are used to maintain strong signal in

Table 1
J^{PC} quantum numbers and their associated meson interpolating fields.

0^{++}	0^{+-}	0^{-+}	0^{--}
$\bar{q}^a q^a$	$\bar{q}^a \gamma_4 q^a$	$\bar{q}^a \gamma_5 q^a$	$-i\bar{q}^a \gamma_5 \gamma_j E_j^{ab} q^b$
$-i\bar{q}^a \gamma_j E_j^{ab} q^b$	$\bar{q}^a \gamma_5 \gamma_j B_j^{ab} q^b$	$\bar{q}^a \gamma_5 \gamma_4 q^a$	
$-\bar{q}^a \gamma_j \gamma_4 \gamma_5 B_j^{ab} q^b$		$-\bar{q}^a \gamma_j B_j^{ab} q^b$	
$-\bar{q}^a \gamma_j \gamma_4 E_j^{ab} q^b$		$-\bar{q}^a \gamma_4 \gamma_j B_j^{ab} q^b$	
1^{++}	1^{+-}	1^{-+}	1^{--}
$-i\bar{q}^a \gamma_5 \gamma_j q^a$	$-i\bar{q}^a \gamma_5 \gamma_4 \gamma_j q^a$	$\bar{q}^a \gamma_4 E_j^{ab} q^b$	$-i\bar{q}^a \gamma_j q^a$
$i\bar{q}^a \gamma_4 B_j^{ab} q^b$	$i\bar{q}^a B_j^{ab} q^b$	$-\epsilon_{jkl} \bar{q}^a \gamma_k B_l^{ab} q^b$	$\bar{q}^a E_j^{ab} q^b$
$i\epsilon_{jkl} \bar{q}^a \gamma_k E_l^{ab} q^b$	$\bar{q}^a \gamma_5 E_j^{ab} q^b$	$\epsilon_{jkl} \bar{q}^a \gamma_4 \gamma_k B_l^{ab} q^b$	$-i\bar{q}^a \gamma_5 B_j^{ab} q^b$
$i\epsilon_{jkl} \bar{q}^a \gamma_k \gamma_4 E_l^{ab} q^b$	$\bar{q}^a \gamma_5 \gamma_4 E_j^{ab} q^b$	$-i\epsilon_{jkl} \bar{q}^a \gamma_5 \gamma_4 \gamma_k E_l^{ab} q^b$	$i\bar{q}^a \gamma_4 \gamma_5 B_j^{ab} q^b$

the two-point correlation functions. Chromo-electric and -magnetic fields are created from APE-smeared links [4] at both the source and sink using the highly-improved $\mathcal{O}(a^4)$-improved lattice field strength tensor [5]. In this study, the smearing fraction $\alpha = 0.7$ (keeping 0.3 of the original link) and the process of smearing and $SU(3)$ link projection is iterated four times [6]. This amount of smearing is sufficient to provide a meaningful topological charge and appears to be suitable for the creation of exotic mesons. As such, the results presented here supersede an earlier presentation of hybrid meson masses [7].

Propagators are generated using the fat-link irrelevant clover (FLIC) fermion action [8] where the irrelevant Wilson and clover operators of the fermion action are constructed using fat links while the relevant operators use the untouched (thin) gauge links. FLIC fermions provide a new form of nonperturbative $\mathcal{O}(a)$ improvement [9,10] where near-continuum results are obtained at finite lattice spacing. Access to the light quark mass regime is enabled by the improved chiral properties of the lattice fermion action [10].

Excited states are extracted using a variational technique, corresponding to a construction of optimal linear combinations of the original operators. For the sake of completeness, we shall discuss this here, in direct analogy to the procedure described in [11].

3. ANALYTICAL PROCESS

Consider the momentum-space meson two-point function for $t > 0$,

$$G_{ij}(t,\vec{p}) = \sum_{\vec{x}} e^{-i\vec{p}\cdot\vec{x}} \langle \Omega | \chi_i(t,\vec{x}) \chi_j^\dagger(0,\vec{0}) | \Omega \rangle \ , \quad (1)$$

where i, j label the different interpolating fields and we focus on Lorentz scalar interpolators for simplicity. At the hadronic level,

$$\begin{aligned} G_{ij}(t,\vec{p}) \ &= \ \sum_{\vec{x}} e^{-i\vec{p}\cdot\vec{x}} \sum_{H,p'} \langle \Omega | \chi_i(t,\vec{x}) | H,p' \rangle \\ &\times \ \langle H,p' | \chi_j^\dagger(0,\vec{0}) | \Omega \rangle \ , \end{aligned}$$

where the $|H,p'\rangle$ are a complete set of hadronic states.

$$\sum_{H,p'} |H,p'\rangle\langle H,p'| = I \ . \quad (2)$$

We can make use of translational invariance to write this as

$$\begin{aligned} &\sum_{\vec{x},H,p'} e^{-i\vec{p}\cdot\vec{x}} \left\langle \Omega \left| \chi_i(0) e^{i\hat{\vec{P}}\cdot\vec{x}} e^{-\hat{H}t} \right| H,p' \right\rangle \times \\ &\left\langle H,p' \left| \chi_j^\dagger(0) \right| \Omega \right\rangle \\ &= \sum_H e^{-E_H t} \left\langle \Omega | \chi_i | H,p \rangle \langle H,p | \chi_j^\dagger | \Omega \right\rangle \ . \quad (3) \end{aligned}$$

It is convenient in the following discussion to label the states which have the χ interpolating field quantum numbers as $|H_\alpha\rangle$ for $\alpha = 1, 2, \cdots, N$. In

general the number of states, N, in this tower of excited states may be infinite, but we will only ever need to consider a finite set of the lowest such states here. After selecting zero momentum, $\vec{p} = 0$,

$$G_{ij}(t) \equiv G_{ij}(t, \vec{0}) = \sum_{\alpha=1}^{N} e^{-m_\alpha t} \lambda_i^\alpha \lambda_j^{\dagger\alpha} \ , \tag{4}$$

where λ_i^α and $\lambda_j^{\dagger\alpha}$ are coefficients denoting the couplings of the interpolating fields χ_i and $\chi_j^\dagger$, respectively, to the state $|H_\alpha\rangle$. If we use identical source and sink interpolating fields then it follows from the definition of the coupling strength that $\lambda_j^{\dagger\alpha} = (\lambda_j^\alpha)^*$ and from Eq. (4) we see that $G_{ij}(t) = [G_{ji}(t)]^*$, i.e., G is a Hermitian matrix. If, in addition, we use only real coefficients in the link products, then G is a real symmetric matrix. For the correlation matrices that we construct we have real link coefficients but we use smeared sources and point sinks and so in our calculations G is a real but non-symmetric matrix. Since G is a real matrix for the infinite number of possible choices of interpolating fields with real coefficients, then we can take λ_i^α and $\lambda_j^{\dagger\alpha}$ to be real coefficients here without loss of generality. In constructing correlation functions, we effectively average over $\{U\}$ and $\{U^*\}$ configurations to ensure λ_i^α is purely real, even on a finite ensemble of gauge field configurations [11].

Now, let us consider the ideal case where we have N interpolating fields with the same quantum numbers, but which give rise to N linearly independent states when acting on the vacuum. In this case we can construct N ideal interpolating source and sink fields which perfectly isolate the N individual hadron states $|H_\alpha\rangle$, i.e.,

$$\phi^{\dagger\alpha} = \sum_{i=1}^{N} u_i^\alpha \ \chi_i^\dagger \ , \tag{5}$$

$$\phi^{\alpha} = \sum_{i=1}^{N} v_i^{*\alpha} \ \chi_i \ , \tag{6}$$

such that

$$\langle H_\beta | \, \phi^{\dagger\alpha} \, |\Omega\rangle = \delta_{\alpha\beta} \ z^{\dagger\alpha} \ , \tag{7}$$

$$\langle \Omega | \, \phi^{\alpha} \, |H_\beta\rangle = \delta_{\alpha\beta} \ z^{\alpha} \ , \tag{8}$$

where z^α and $z^{\dagger\alpha}$ are the coupling strengths of ϕ^α and $\phi^{\dagger\alpha}$ to the state $|H_\alpha\rangle$. The coefficients u_i^α and $v_i^{*\alpha}$ in Eqs. (3) may differ when the source and sink have different smearing prescriptions, again indicated by the differentiation between z^α and $z^{\dagger\alpha}$ (recall z is real).

For notational convenience for the remainder of this discussion repeated indices i, j, k are to be understood as being summed over, whereas α denoting a particular state is not. At $\vec{p} = 0$, it follows that,

$$\begin{aligned} G_{ij}(t) \ u_j^\alpha &= \left(\sum_{\vec{x}} \langle \Omega | \, \chi_i \chi_j^\dagger \, |\Omega\rangle \right) u_j^\alpha \\ &= \lambda_i^\alpha z^{\dagger\alpha} e^{-m_\alpha t}. \end{aligned} \tag{9}$$

The t-dependence in this expression is purely in the exponential term, leading to the recurrence relationship

$$G_{ij}(t) \, u_j^\alpha = e^{m_\alpha} G_{ik}(t+1) \, u_k^\alpha \ , \tag{10}$$

which can be rewritten as

$$[G(t+1)]^{-1}_{ki} G_{ij}(t) \, u_j^\alpha = e^{m_\alpha} \ u_k^\alpha \ . \tag{11}$$

This is the generalized eigenvalue equation for $[G(t+1)]^{-1} G(t)$ with eigenvalues e^{m_α} and eigenvectors u^α. Hence the natural logarithms of the eigenvalues of $[G(t+1)]^{-1} G(t)$ are the masses of the N hadrons in the tower of excited states for the given quantum numbers . The eigenvectors are the coefficients of the χ fields providing the optimal linear combination for that state.

One can also construct the equivalent left-eigenvalue equation to recover the v vectors, providing the optimal linear combination of annihilation interpolators,

$$v_k^{*\alpha} G_{kj}(t) = e^{m_\alpha} v_i^{*\alpha} G_{ij}(t+1) \ . \tag{12}$$

Recalling Eq. (9), one finds:

$$G_{ij}(t) \ u_j^\alpha = z^{\dagger\alpha} \lambda_i^\alpha e^{-m_\alpha t} \ , \tag{13}$$

$$v_i^{*\alpha} \ G_{ij}(t) = z^\alpha \lambda_j^{\dagger\alpha} e^{-m_\alpha t} \ , \tag{14}$$

$$v_k^{*\alpha} \ G_{kj}(t) G_{il}(t) \ u_l^\alpha = z^\alpha z^{\dagger\alpha} \lambda_i^\alpha \lambda_j^{\dagger\alpha} e^{-2m_\alpha t} \tag{15}$$

The definitions of Eqs. (7) and (8) imply

$$v_i^{*\alpha} \ G_{ij}(t) \ u_j^\alpha = z^\alpha z^{\dagger\alpha} e^{-m_\alpha t}, \tag{16}$$

indicating the eigenvectors may be used to construct a correlation function in which a single state mass $m_\alpha$is isolated and which can be analyzed using the methods of Section II. We refer to this as the projected correlation function in the following. Combining Eqs. (15) and (16) leads us to the result

$$\frac{v_k^{*\alpha}\ G_{kj}(t)G_{il}(t)\ u_l^\alpha}{v_k^{*\alpha}G_{kl}(t)u_l^\alpha} = \lambda_i^\alpha \lambda_j^{\dagger\alpha} e^{-m_\alpha t}\ . \qquad (17)$$

By extracting all N^2 such ratios, we can exactly recover all of the real couplings λ_i^α and $\lambda_j^{\dagger\alpha}$ of χ_i and $\chi_j^\dagger$ respectively to the state $|H_\alpha\rangle$.

Note that throughout this section no assumptions have been made about the symmetry properties of G_{ij}. This is essential due to our use of smeared sources and point sinks.

In practice we will only have a relatively small number, $M < N$, of interpolating fields in any given analysis. These M interpolators should be chosen to have good overlap with the lowest M excited states in the tower and we should attempt to study the ratios in Eq. (17) at early to intermediate Euclidean times, where the contribution of the $(N - M)$ higher mass states will be suppressed but where there is still sufficient signal to allow the lowest M states to be seen. This procedure will lead to an estimate for the masses of each of the lowest M states in the tower of excited states. Of these M predicted masses, the highest will in general have the largest systematic error while the lower masses will be the most reliably determined. Repeating the analysis with varying M and different combinations of interpolating fields will give an objective measure of the reliability of the extraction of these masses.

In our case of a modest 2×2 correlation matrix ($M = 2$) we take a cautious approach to the selection of the eigenvalue analysis time. As already explained, we perform the eigenvalue analysis at an early to moderate Euclidean time where statistical noise is suppressed and yet contributions from at least the lowest two mass states is still present. One must exercise caution in performing the analysis at too early a time, as more than the desired $M = 2$ states may be contributing to the 2×2 matrix of correlation functions.

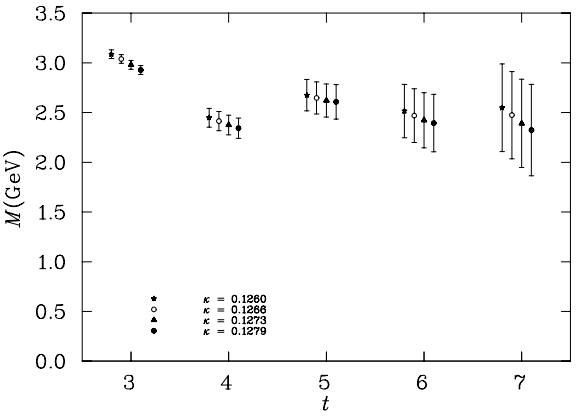

Figure 1. Effective mass plot of the 1^{-+} exotic meson obtained from the hybrid interpolating field $\epsilon_{jkl}\bar{q}^a\gamma_k B_l^{ab} q^b$.

4. RESULTS

The following results are based on 110 mean-field $\mathcal{O}(a^2)$-improved Luscher-Weisz [12] gauge fields on a $16^3 \times 32$ lattice at $\beta = 4.60$ providing a lattice spacing of $a = 0.122(2)$ fm set by the string tension $\sqrt{\sigma} = 440$ MeV.

Of the hybrid interpolators listed in Table 1, only the interpolating fields merging the large spinor components of the quark and antiquark fields provide a clear mass plateau. The effective mass plot for the exotic 1^{-+} meson is illustrated in Fig. 1, where a plateau at early times is observed confirming the existence of the exotic 1^{-+}.

Figures 2 and 3 illustrate the effective masses $M(t) = -\log(G(t+1)/G(t))$, obtained from the first and third, and second and fourth, pion (0^{-+}) interpolators of Table 1 for our intermediate quark mass ($m_\pi^2 \sim 0.6$ GeV^2). Excellent agreement is seen between the standard and hybrid interpolator-based correlation functions. Similar results are seen in Fig. 4 comparing effective masses obtained from the first and third ρ-meson (1^{--}) interpolators of Table 1.

Table 2 summarizes these preliminary results, and table 3 presents a further preliminary calculation of a pion excited state mass, using the first two pion operators listed above.

Further work on this topic will focus on increasing the statistics, and increasing the number of operators used in the variational process.

Table 2
Meson masses as a function of the hopping parameter κ.

J^{PC}	Operator	Mass(GeV) $\kappa = 0.1260$	$\kappa = 0.1266$	$\kappa = 0.1273$	$\kappa = 0.1279$	$\kappa = 0.1286$
$\pi: 0^{-+}$	$\bar{q}^a\gamma_5 q^a$	$0.965 \pm .006$	$0.887 \pm .006$	$0.789 \pm .007$	$0.696 \pm .007$	$0.570 \pm .008$
	$\bar{q}^a\gamma_5\gamma_4 q^a$	$0.957 \pm .005$	$0.879 \pm .005$	$0.781 \pm .005$	$0.688 \pm .006$	$0.563 \pm .006$
	$-\bar{q}^a\gamma_j B_j^{ab} q^b$	$0.998 \pm .030$	$0.916 \pm .031$	$0.813 \pm .031$	$0.717 \pm .032$	$0.589 \pm .035$
	$-\bar{q}^a\gamma_4\gamma_j B_j^{ab} q^b$	$0.984 \pm .033$	$0.902 \pm .034$	$0.800 \pm .035$	$0.704 \pm .037$	$0.575 \pm .039$
$b_1: 1^{+-}$	$-i\bar{q}^a\gamma_5\gamma_4\gamma_j q^a$	$1.713 \pm .018$	$1.671 \pm .019$	$1.623 \pm .021$	$1.583 \pm .022$	$1.541 \pm .026$
	$i\bar{q}^a B_j^{ab} q^b$	$1.685 \pm .205$	$1.621 \pm .226$	$1.525 \pm .275$	$1.398 \pm .353$	$1.120 \pm .500$
$\rho: 1^{--}$	$-i\bar{q}^a\gamma_j q^a$	$1.212 \pm .009$	$1.157 \pm .010$	$1.093 \pm .012$	$1.037 \pm .014$	$0.973 \pm .019$
	$\bar{q}^a E_j^{ab} q^b$	$1.198 \pm .056$	$1.151 \pm .063$	$1.099 \pm .076$	$1.048 \pm .091$	$0.958 \pm .110$
	$-i\bar{q}^a\gamma_5 B_j^{ab} q^b$	$1.214 \pm .050$	$1.156 \pm .053$	$1.085 \pm .058$	$1.018 \pm .064$	$0.922 \pm .077$
	$i\bar{q}^a\gamma_4\gamma_5 B_j^{ab} q^b$	$1.125 \pm .049$	$1.060 \pm .054$	$0.982 \pm .061$	$0.907 \pm .069$	$0.799 \pm .087$
1^{-+}	$-\epsilon_{jkl}\bar{q}^a\gamma_k B_l^{ab} q^b$	$2.519 \pm .186$	$2.483 \pm .192$	$2.450 \pm .200$	$2.434 \pm .207$	$2.430 \pm .211$

Table 3
Pion excited state from variational analysis.

	Mass(GeV) $\kappa = 0.1260$	$\kappa = 0.1266$	$\kappa = 0.1273$	$\kappa = 0.1279$	$\kappa = 0.1286$
$\pi(1):$	$0.956 \pm .007$	$0.878 \pm .007$	$0.779 \pm .008$	$0.684 \pm .009$	$0.555 \pm .014$
$\pi(2):$	$1.889 \pm .064$	$1.819 \pm .070$	$1.730 \pm .080$	$1.647 \pm .096$	$1.548 \pm .141$

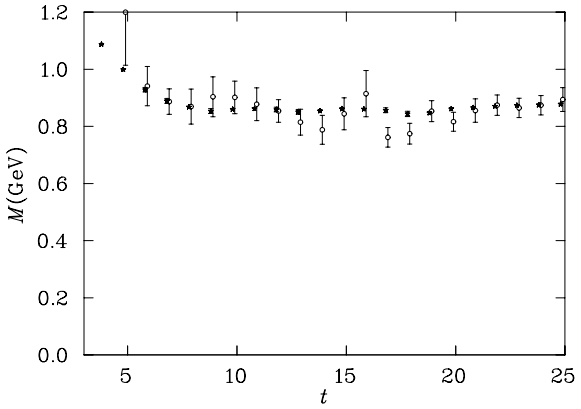

Figure 2. Effective mass plot for correlation functions of the standard pion interpolator $\bar{q}^a\gamma_5 q^a$ and the hybrid pion interpolator $\bar{q}^a\gamma_j B_j^{ab} q^b$.

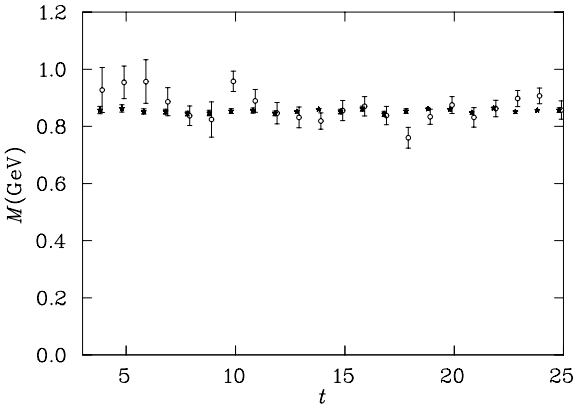

Figure 3. Effective mass plot for correlation functions of the standard axial-vector pion interpolator $\bar{q}^a\gamma_5\gamma_4 q^a$ and the hybrid pion interpolator $\bar{q}^a\gamma_4\gamma_j B_j^{ab} q^b$.

5. ACKNOWLEDGMENTS

This research is supported by the Australian National Computing Facility for Lattice Gauge Theory and the Australian Research Council.

REFERENCES

1. C. Michael, [hep-ph/0308293], and references therein.
2. S. Gusken, Nucl. Phys. Proc. Suppl. **17**, 361

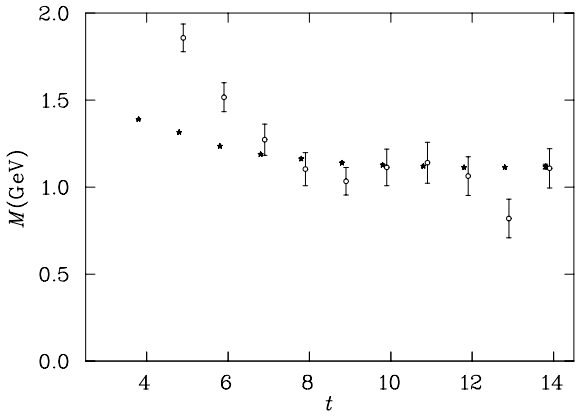

Figure 4. Effective mass plot for correlation functions of the standardρ-meson interpolator $\bar{q}^a\gamma_j q^a$ and the hybrid ρ interpolator $\bar{q}^a\gamma_4\gamma_5 B_j^{ab} q^b$.

(1990).
3. J. M. Zanotti, *et al.*, to appear in Phys. Rev. D, [hep-lat/0304001].
4. M. Falcioni *et al.*, Nucl. Phys. **B251** (1985) 624; M. Albanese *et al.*, Phys. Lett. B **192** (1987) 163.
5. S. O. Bilson-Thompson, *et al.*, Annals Phys. **304** (2003) 1 [hep-lat/0203008].
6. F.D. Bonnet *et al.*, Phys. Rev. D **62** (2000) 094509 [hep-lat/0001018].
7. J. N. Hedditch, D. B. Leinweber, A. G. Williams and J. M. Zanotti, hep-lat/0309119.
8. J.M. Zanotti *et al.*, Phys. Rev. D **60** (2002) 074507 [hep-lat/0110216].
9. D. B. Leinweber, *et al.*, [nucl-th/0211014].
10. J. Zanotti, *et al.*, in preparation.
11. W. Melnitchouk *et al.*, Phys. Rev. D **67** (2003) 114506 [hep-lat/0202022].
12. M. Luscher and P. Weisz, Commun. Math. Phys. **97**, 59 (1985) [ibid. **98**, 433 (1985)].